


# Electric modulation of anisotropic magnetoresistance in Pt/$HfO_{2-x}$/$NiO_y$/Ni heterojunctions

Xiaoyu Ye(叶晓羽), Xiaojian Zhu(朱小健), Huali Yang(杨华礼), Jipeng Duan(段吉鹏), Cui Sun(孙翠), and Run-Wei Li(李润伟)

**Citation:**Chin. Phys. B, 2023, 32 (**8**): 087305. DOI: 10.1088/1674-1056/acd2b6
Journal homepage: http://cpb.iphy.ac.cn; http://iopscience.iop.org/cpb

**What follows is a list of articles you may be interested in**

---

## Sign reversal of anisotropic magnetoresistance and anomalous thickness-dependent resistivity in $Sr_2CrWO_6$/$SrTiO_3$ films

Chunli Yao(姚春丽), Tingna Shao(邵婷娜), Mingrui Liu(刘明睿), Zitao Zhang(张子涛), Weimin Jiang(姜伟民), Qiang Zhao(赵强), Yujie Qiao(乔宇杰), Meihui Chen(陈美慧), Xingyu Chen(陈星宇), Ruifen Dou(窦瑞芬), Changmin Xiong(熊昌民), and Jiacai Nie(聂家财)

Chin. Phys. B, 2022, 31 (**10**): 107302. DOI: 10.1088/1674-1056/ac6164

## Anomalous anisotropic magnetoresistance in single-crystalline Co/$SrTiO_3$(001) heterostructures

Shuang-Long Yang(杨双龙), De-Zheng Yang(杨德政), Yu Miao(缪宇), Cun-Xu Gao(高存绪), and De-Sheng Xue(薛德胜)

Chin. Phys. B, 2021, 30 (**12**): 127302. DOI: 10.1088/1674-1056/ac05ad

## Ferroelectric effect and equivalent polarization charge model of $PbZr_{0.2}Ti_{0.8}O_3$ on AlGaN/GaN MIS-HEMT

Yao-Peng Zhao(赵垚澎), Chong Wang(王冲), Xue-Feng Zheng(郑雪峰), Xiao-Hua Ma(马晓华), Ang Li(李昂), Kai Liu(刘凯), Yun-Long He(何云龙), Xiao-Li Lu(陆小力) and Yue Hao(郝跃)

Chin. Phys. B, 2021, 30 (**5**): 057302. DOI: 10.1088/1674-1056/abd469

## Implementation of synaptic learning rules by $TaO_x$ memristors embedded with silver nanoparticles

Yue Ning(宁玥), Yunfeng Lai(赖云锋), Jiandong Wan(万建栋), Shuying Cheng(程树英), Qiao Zheng(郑巧), and Jinling Yu(俞金玲)

Chin. Phys. B, 2021, 30 (**4**): 047301. DOI: 10.1088/1674-1056/abccb8

## Comparative study on characteristics of Si-based AlGaN/GaN recessed MIS-HEMTs with $HfO_2$ and $Al_2O_3$ gate insulators

Yao-Peng Zhao(赵垚澎), Chong Wang(王冲), Xue-Feng Zheng(郑雪峰), Xiao-Hua Ma(马晓华), Kai Liu(刘凯), Ang Li(李昂), Yun-Long He(何云龙), Yue Hao(郝跃)

Chin. Phys. B, 2020, 29 (**8**): 087304. DOI: 10.1088/1674-1056/ab8daa

---

**RAPID COMMUNICATION**

# Electric modulation of anisotropic magnetoresistance in Pt/$HfO_{2-x}$/$NiO_y$/Ni heterojunctions

Xiaoyu Ye(叶晓羽)[1,2,3], Xiaojian Zhu(朱小健)[1,2,3,†], Huali Yang(杨华礼)[1,2], Jipeng Duan(段吉鹏)[1,2,3], Cui Sun(孙翠)[1,2], and Run-Wei Li(李润伟)[1,2,3,‡]

[1] *CAS Key Laboratory of Magnetic Materials and Devices, Ningbo Institute of Materials Technology and Engineering, Chinese Academy of Sciences, Ningbo* 315201, *China*

[2] *Zhejiang Province Key Laboratory of Magnetic Materials and Application Technology, Ningbo Institute of Materials Technology and Engineering, Chinese Academy of Sciences, Ningbo* 315201, *China*

[3] *College of Materials Science and Opto-Electronic Technology, University of Chinese Academy of Sciences, Beijing* 100049, *China*

(Received 10 April 2023; revised manuscript received 29 April 2023; accepted manuscript online 5 May 2023)

Electric field control of magnetism through nanoionics has attracted tremendous attention owing to its high efficiency and low power consumption. In solid-state dielectrics, an electric field drives the redistribution of ions to create one-dimensional magnetic conductive nanostructures, enabling the realization of intriguing magnetoresistance (MR) effects. Here, we explored the electric-controlled nickel and oxygen ion migration in Pt/$HfO_{2-x}$/$NiO_y$/Ni heterojunctions for MR modulation. By adjusting the voltage polarity and amplitude, the magnetic conductive filaments with mixed nickel and oxygen vacancy are constructed. This results in the reduction of device resistance by $\sim 10^3$ folds, and leads to an intriguing partial asymmetric MR effect. We show that the difference of the device resistance under positive and negative saturation magnetic fields exhibits good linear dependence on the magnetic field angle, which can be used for magnetic field direction detection. Our study suggests the potential of electrically controlled ion migration in creating novel magnetic nanostructures for sensor applications.

**Keywords:** nanoionics, resistance random access memory, anisotropic magnetoresistance, angle detection

**PACS:** 73.40.Rw, 75.47.–m, 81.05. –t, 81.15.Jj **DOI:** 10.1088/1674-1056/acd2b6

## 1. Introduction

Electric control of magnetism has attracted tremendous attention in the past decades owing to its importance in the development of various spintronic devices used in memories, logic devices, sensors, etc.[1–5] Compared with the conventional methods by exploiting high-density electric current for magnetism modulation,[6–8] electric-controlled ions transportation and related electrochemical reactions at the nanoscale in solid-state dielectric tune the magnetism with much-enhanced efficiencies.[9–13] In resistive switching (RS) device with a structure of electrode/dielectric/electrode, the electric field can drive the migration of ions (e.g., $O^{2-}$, $Ag^{2+}$, etc.) and construct one-dimension conductive nanostructures, such as oxygen vacancy (Vo) and Ag filaments.[14–20] Particularly, when magnetic materials are selected as electrodes (e.g., Ni,[21] Co, etc.[22,23]) or dielectrics (e.g., $Ga_2O_3$,[24] NiO, etc.[25]), the magnetic nanostructure exhibiting distinct magnetoresistance (MR) effects can be obtained. While previous studies focused on single-type ion manipulations, recent studies showed that it was possible to drive the movement of different types of ions (e.g., $O^{2-}$, $Ag^{2+}$, etc.)[26] in the same heterojunctions, offering opportunities for the establishment of one-dimensional nanostructures with diverse compositions and magnetism for the exploration of intriguing MR effects.

Here, we report the electric field control of oxygen and nickel ion migration in the Pt/$HfO_{2-x}$/$NiO_y$/Ni device for MR modulation. We show that the one-dimensional nanostructure with mixed Vo and Ni filaments could be constructed via electric field induced ion migration. The formed nanostructure reduced the device resistance by $\sim 10^3$ folds and led to unconventional anisotropic magnetoresistance (AMR) effect due to the magnetic coupling effect at the $NiO_y$/Ni interface. We investigated the angle-dependent MR asymmetry of the nanostructures, and showcased its potential application as a magnetic sensor for detecting the magnetic field direction. This work contributes to a deeper insight into the electric-controlled ion migration in magnetic heterojunctions and provides a versatile approach for the exploration of novel MR effects enabled by nanoionics.

## 2. Experimental details

Figure 1(a) shows the schematic diagram of the device structure, i.e., Pt/$HfO_{2-x}$/$NiO_y$/Ni. The Ni bottom electrode and Pt top electrode were deposited by electron beam evap-

†Corresponding author. E-mail: zhuxj@nimte.ac.cn
‡Corresponding author. E-mail: runweili@nimte.ac.cn

© 2023 Chinese Physical Society and IOP Publishing Ltd 

oration at a pressure of $\sim 2 \times 10^{-5}$ Pa. The $NiO_y$ film was formed by oxidizing the Ni film under a vertical external magnetic field. The $HfO_{2-x}$ film was deposited by magnetron sputtering in a mixed atmosphere of Ar and $O_2$ with a ratio of 1:4 at a pressure of 0.9–1.0 Pa, where the radio frequency power was fixed at 60 W. The device size was $100 \times 100$ μm$^2$, patterned by ultraviolet lithography and lift-off processes. Figure 1(b) shows the scanning electron microscope (SEM) image and transmission electron microscopy (TEM) results of the device. As can be seen, both the $HfO_{2-x}$ and $NiO_y$ layers were amorphous and had a thickness of $\sim 4$ nm. Additionally, high-angle annular dark field (HAADF) and energy dispersive spectroscopy (EDS) were taken to analyze the elementary distribution in the device. The results are shown in Figs. 1(c) and 1(d). The atomic fractions of O/Ni/Hf atoms at the corresponding positions as marked in the $HfO_{2-x}/NiO_y$ bilayers were estimated, indicating that the stoichiometry of $HfO_{2-x}$ and $NiO_y$ layers were 1:2.23 and 1:0.9, respectively.

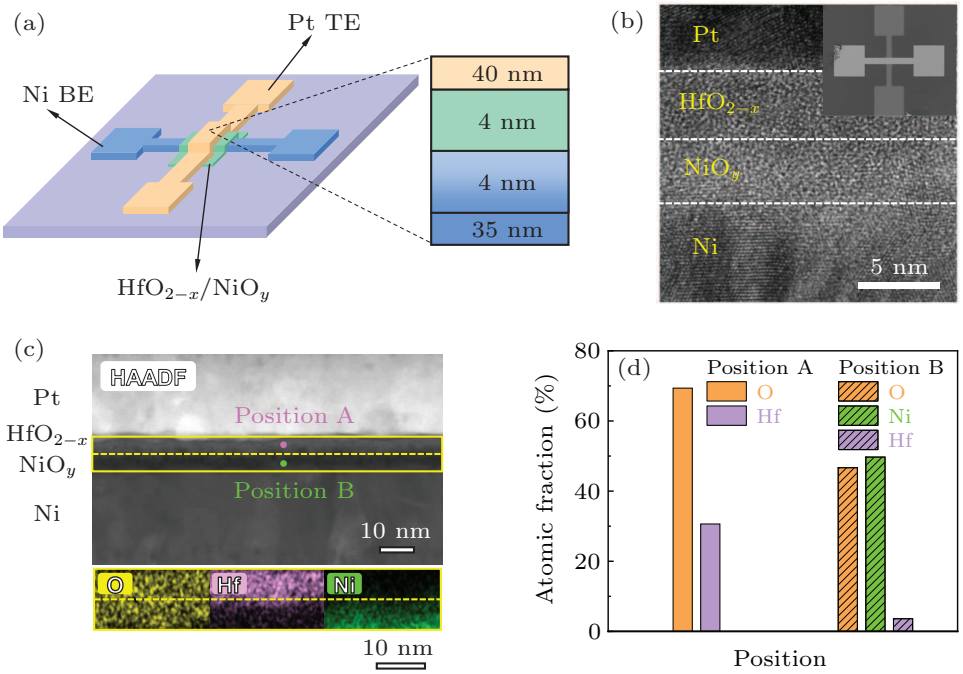



**Fig. 1.** (a) Schematic diagram of the Pt/$HfO_{2-x}$/$NiO_y$/Ni device arranged in a crossbar structure. (b) Cross-sectional HRTEM image of the device. Inset: Top-view SEM image. (c) Mapping of the element distributions in the device. (d) Atomic fraction of O/Ni/Hf atoms of different positions as marked in (c).

## 3. Results and discussion

### 3.1. Electric programming of the magnetic heterojunction

According to the previous studies, applying positive voltages on the Ni electrode can lead to Ni oxidization and inject $Ni^{2+}$ ions into the oxide layers, causing the formation of Ni filament.[27–30] On the other hand, the $O^{2-}$ in $HfO_{2-x}$ can also be driven to form Vo filament.[31–34] Therefore, by carefully controlling the voltage application conditions through the above two steps, one may create filaments with mixed element compositions in the Pt/$HfO_{2-x}$/$NiO_y$/Ni device. We monitored the current evolution during the application of sweeping voltages, and the current–voltage ($I$–$V$) characteristics is shown in Fig. 2(a). Specifically, the as-fabricated device had an initial high resistance state (HRS) of $\sim 10^{10}$ Ω. When a positive sweeping voltage was applied on the Pt electrode with Ni electrode grounded, the current passing through the device jumped abruptly to the preset compliance current ($I_{cc1} = 10$ μA) at $\sim 0.71$ V, changing the device resistance to an intermediate resistance state (IRS) ($\sim 7 \times 10^4$ Ω) (red curve in Fig. 2(a)). This observation was consistent with the formation of Vo based filaments in the $HfO_2$ film.[31] The device resistance was found to be larger than that of the single-atom conductive filament ($\sim 12$ kΩ), indicating that the Vo filament was partially formed. Afterward, we applied a positive sweeping voltage to the Ni electrode with Pt electrode grounded, the device current jumped to a higher compliance current ($I_{cc2} = 250$ μA) at $\sim -1.04$ V, changing the device resistance to a low resistance state (LRS) ($\sim 10^3$ Ω) (blue curve in Fig. 2(a)). Owing to the lower activation energy of $Ni^{2+}$ ions compared with $O^{2-}$ ions, $Ni^{2+}$ ions were expected to migrate dominantly and formed Ni filaments in this stage.[35,36] Therefore, the two-step programming of the device through controlling the voltage polarity and intensity was expected to form conductive filaments (CFs) with mixed Vo and Ni, leading to successful construction of the Pt/Hf-CF/$NiO_y$/Ni-CF/Ni nanostructure in the device. After removing the programming voltage, the device resistance was reduced by $\sim 10^3$, and the LRS can be maintained for over $10^4$ s, indicating the good stability of the nanostructure.

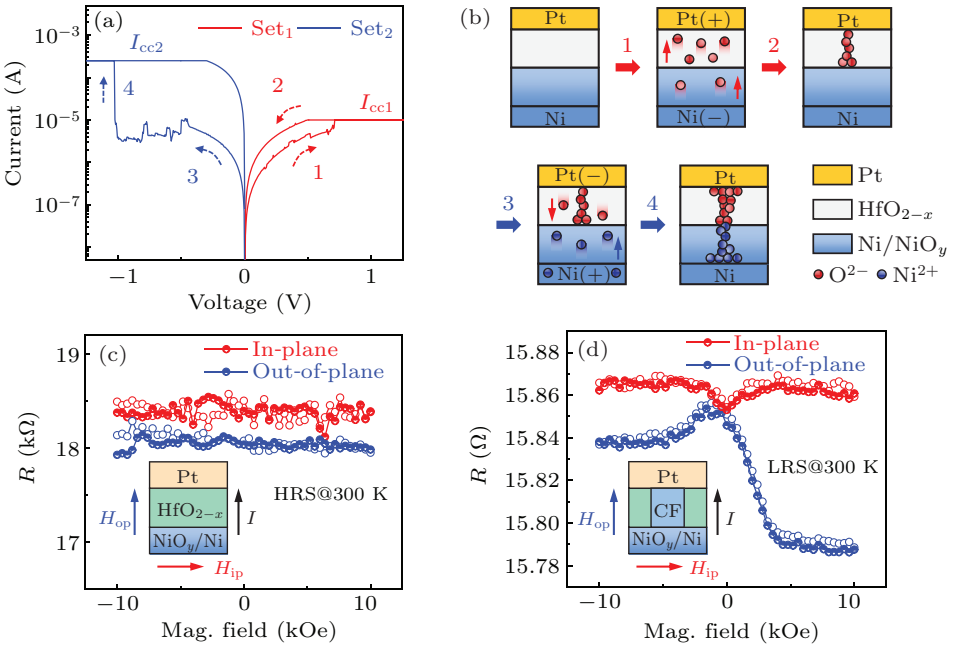



**Fig. 2.** (a) The *I*–*V* curves of the Pt/$HfO_{2-x}$/$NiO_y$/Ni heterojunction. (b) The cartoons showing hypothesized ion migration processes in the device. (c)–(d) MR behaviors with the magnetic field applied along the in-plane and out-of-plane direction for the device (c) before and (d) after electric programming. Inset: Setup showing the applied current and magnetic field direction during MR measurements.

### 3.2. Magnetoresistance behavior measurements

The MR properties of the Pt/$HfO_{2-x}$/$NiO_y$/Ni device before and after electrical programming were studied. The measurements were carried out using the standard four-probe method in a physical property measurement system (PPMS) at room temperature. A constant current of 10 μA was applied and the resistance was recorded with the following magnetic field sweep sequences: $10 \to 0 \to -10 \to 0 \to 10$ kOe. The MR curves were recorded with the magnetic field applied along the in-plane and out-of-plane directions, respectively. The measurement configurations are shown in the inset of Figs. 2(c) and 2(d). The MR ratio was calculated as

$$\frac{\Delta R}{R_0} = \frac{R_H - R_0}{R_0}, \tag{1}$$

where $R_H$ and $R$ correspond to the resistance recorded at the field strength of $H$ and zero field, respectively. The MR curves retraced as the field swept from positive to negative then backward. As can be seen from Fig. 2(c), the as-fabricated Pt/$HfO_{2-x}$/$NiO_y$/Ni device without electric programming was insensitive to the magnetic intensity and direction. In contrast, an apparent MR anisotropy was clearly observed in the Pt/$HfO_{2-x}$/$NiO_y$/Ni device after electric stimuli, as shown in Fig. 2(d). For magnetic field applied in the out-of-plane direction, the MR value decreased under a negative (positive) magnetic field up to ∼ −4 kOe (∼ 4.8 kOe) and approached saturation thereafter, showing partial MR asymmetry (blue curves in Fig. 2(d)). On the other hand, as the magnetic field was applied in the film plane, the MR curve possessed good symmetry (red curves in Fig. 2(d)).

#### 3.2.1. Temperature dependent magnetoresistance behaviors

Figure 3 shows the temperature dependence of the MR behavior with magnetic field applied in the out-of-plane and in-plane directions, respectively. Figure 3(a) displays the MR curves with magnetic field along the out-of-plane direction. As can be seen, the device persisted a partial MR asymmetry feature in the measured temperature range from 300 K to 5 K. Prior further analysis, we decomposed the partial asymmetrical MR curves into symmetric (component 1) and asymmetric (component 2) parts as follows:

$$\text{Symmetric MR} = \frac{\text{MR}_{H+} + \text{MR}_{H-}}{2}, \tag{2}$$

$$\text{Asymmetric MR} = \frac{\text{MR}_{H+} - \text{MR}_{H-}}{2}. \tag{3}$$

As shown in Figs. 3(b) and 3(c), the asymmetric MR exhibited nearly linear dependence on the magnetic field between roughly −4.4 kOe and 4.4 kOe at 300 K, while the symmetric part showed a rapid drop of MR in the low-field region (between −4 kOe and 4 kOe) at 300 K. In both cases, the MR curves became saturated at higher fields. The saturation magnetic fields corresponding to asymmetric MR and symmetric MR gradually decreased at reduced temperature, reaching ∼ 1.8 kOe and ∼ 2.2 kOe at 5 K, respectively. The MR value of the asymmetric part at the saturation magnetic field was nearly constant (∼ 0.14%), which was insensitive to temperature (red dot curve in Fig. 3(d)). The MR value of the symmetric part at saturation magnetic field was calculated to be ∼ −0.24% at 300 K and its amplitude slightly decreased with reduced temperature (black dot curve in Fig. 3(d)). Figure 3(e) shows the MR curves obtained with magnetic field applied in the film plane between 300 K and 5 K. Similar to the

out-of-plane case, the MR increased steeply at low magnetic field and gradually reached saturation at higher fields, yet the MR curves were much more symmetric. The maximum MR value increased from $\sim 0.04\%$ at 300 K to $\sim 0.3\%$ at 5 K, and a steeper increase of the low-field MR was evidenced at reduced temperature, which could be caused by the enhanced spin scattering at low temperature (Fig. 3(f)). Notably, the difference between the MR value at $H = -10$ kOe and 10 kOe kept constant ($\sim 0.3\%$) in out-of-plane direction as shown in Fig. 3(g), demonstrating its weak dependence on temperature.

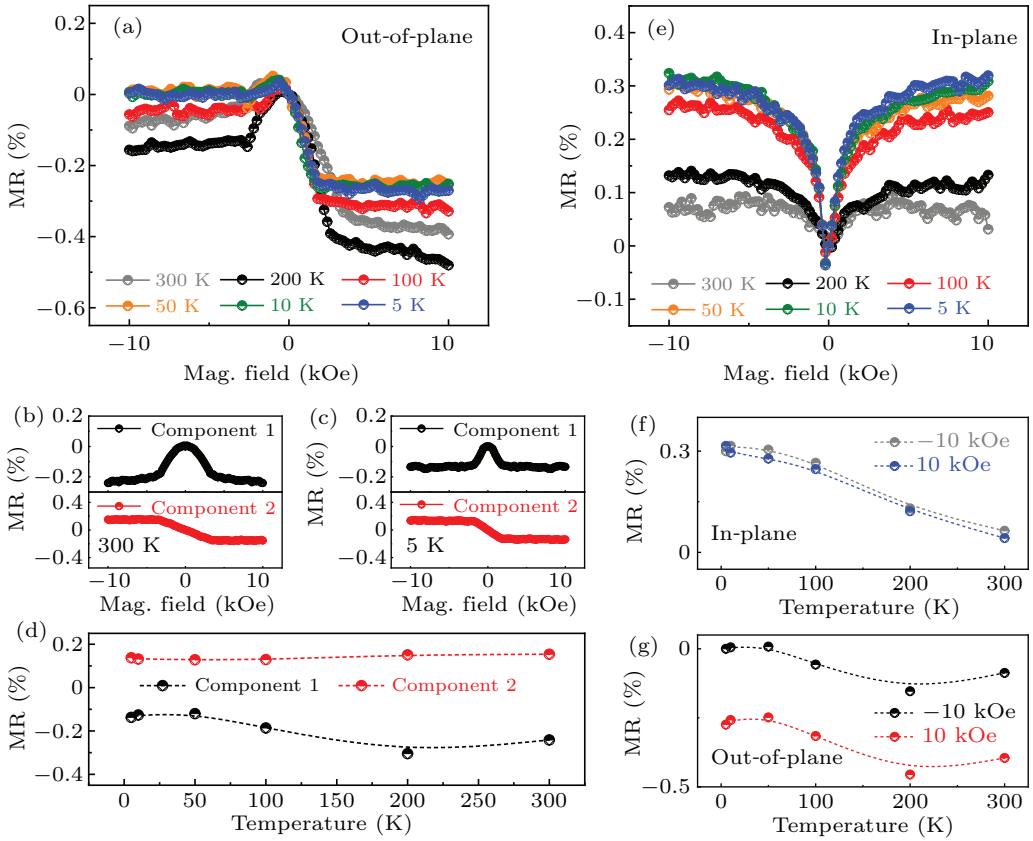



**Fig. 3.** (a) The MR curves measured at different temperatures with the magnetic field along the out-of-plane direction. (b)–(c) The MR curves showing full symmetry (component 1) and asymmetry (component 2), decomposed from (a). (d) Temperature dependence of the symmetric and asymmetric MR values. (e) The MR curves measured at different temperatures with the magnetic field along the in-plane direction. (f)–(g) The evolution of the MR value with temperature with the magnetic field applied along the (f) in-plane and (g) out-of-plane directions.

Based on the above results, the mechanism of the intriguing partial asymmetric MR behavior of Pt/$HfO_{2-x}$/$NiO_y$/Ni heterojunction was analyzed. According to previous studies, the $NiO_y$/Ni interface[37,38] and Ni nanowires[21,39,40] show an asymmetric MR and symmetric MR under magnetic field, respectively, which well matches with the MR behavior of symmetric MR and asymmetric MR components. Therefore, the Pt/$HfO_{2-x}$/$NiO_y$/Ni device showing a partial asymmetric MR could be resulted from the combined magnetic coupling of the $NiO_y$/Ni interface and the nanofilament made of Vo and Ni. Notably, the asymmetric MR originating from $NiO_y$/Ni interface was induced by the out-of-plane spin orientation produced by the external upward magnetic field applied during the growth of the $NiO_y$ layer in fabrication processes, where the spin moment of the ferromagnetic Ni was pinned by the antiferromagnetic (AFM) moment of the $NiO_y$. This characteristic induced a magnetic field direction-dependent carrier transmission efficiency at the $NiO_y$/Ni interface and resulted in the MR with full asymmetry. The value of saturated asymmetric MR which was insensitive to temperature also supported this hypothesis,[41] and it was apparently different from the normal MR which was greatly affected by the temperature. Similar results have also been reported in other AFM/FM interfaces such as Ni–Mn–$X$ ($X$ = In, Ga) system.[42,43]

### 3.2.2. Anisotropic magnetoresistance behaviors

The AMR measurements were conducted to further reveal the unsymmetric MR behavior (Fig. 4). During the AMR measurements, the resistance was recorded by rotating the devices from $\theta = 0°$ to $\theta = 360°$ in the $y$–$z$ plane at room temperature, as shown in Fig. 4(a), where $\theta$ was defined as the angle between the external magnetic field and current flow direction. For instance, $\theta = 0°$ and 90° refer to the out-of-plane and in-plane directions, respectively. Figure 4(b) shows the AMR curve at different temperatures. It can be clearly seen that the device maintains the asymmetry MR behavior from 300 K down to 5 K, rendering a relatively good stability against temperature variation, and ensuring a wide range of

working temperature. Figure 4(c) plots the AMR curves under different magnetic fields (10, 1, 0.1, −0.1, −1, −10 kOe) at 300 K and 5 K. As shown in the upper panel of Fig. 4(c), the AMR curves under 0.1 kOe and 1 kOe almost overlapped thus showed negligible asymmetry, whereas the MR curves deviated from symmetry as the magnetic field increased to 10 kOe. In contrast, the MR asymmetry became more significant under small magnetic fields as the temperature reduced (lower panel of Fig. 4(c)).

Figures 4(d) and 4(e) show the MR curves by sweeping the magnetic field from 10 → 0 → −10 → 0 → 10 kOe at various $\theta$ (from 0° to 360° with an interval of 15°). It was found that when $\theta$ increased from 0° to 90° (i.e., the magnetic field changes from the out-of-plane direction to the in-plane direction), the partial asymmetrical MR behavior diminished and the MR curves became increasingly symmetric as shown in Fig. 4(d). On the other hand, when $\theta$ further increased from 90° to 180°, the partial asymmetrical MR behavior reappeared gradually as $\theta$ increased (Fig. 4(e)). These results indicate that the difference of the device resistance under positive and negative saturation magnetic field was highly sensitive to the angle $\theta$ with good linearity, as shown in Fig. 4(f). The magnetic field sensors based on the AMR effect show linear response to the external magnetic field, allowing for magnetic field direction detection and navigation purposes. The sensor also shows great potential in scaling down and integrating multifunctional applications. Overall, our work demonstrates the feasibility of creating one-dimensional magnetic nanostructures through dual-ion modulation and the generation of unique MR effects that can find diverse applications.

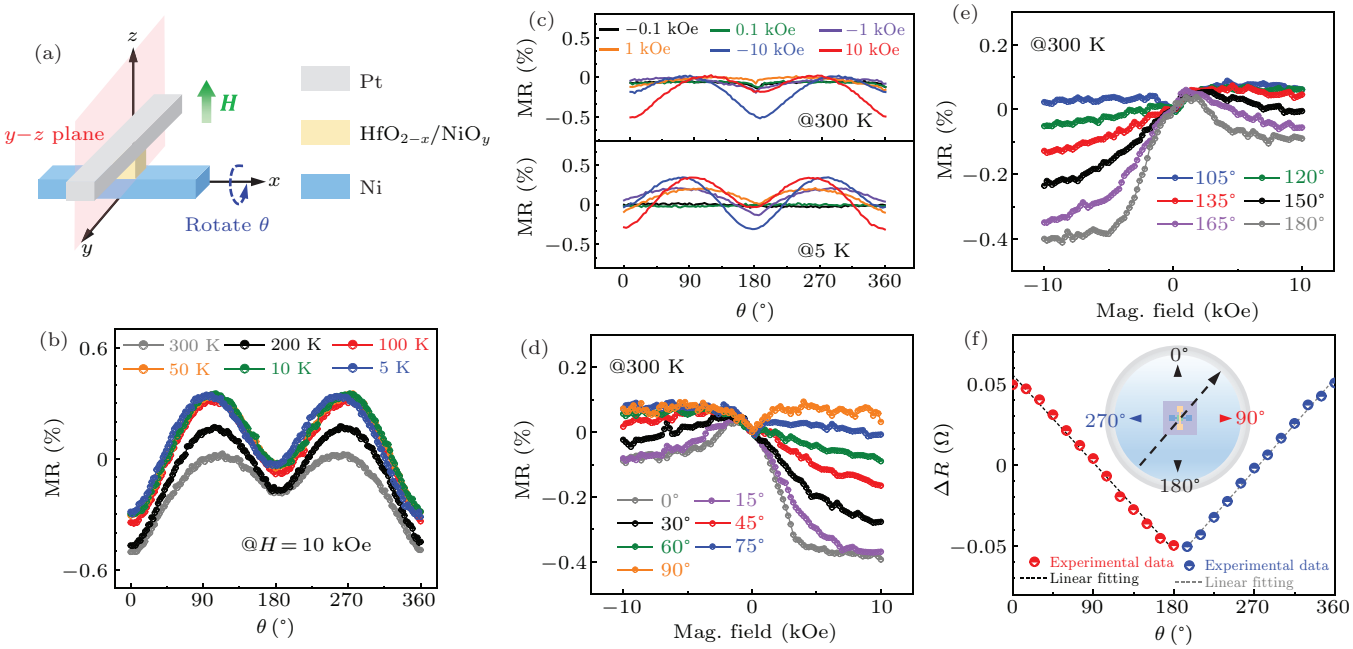



**Fig. 4.** (a) Experimental setup for angle dependent MR measurements. $\theta$ is defined as the angle between the direction of the external magnetic field and the current flow through the device. (b) Angle dependent MR behaviors at $H = 10$ kOe and different temperatures. (c) Angle dependent MR behaviors under different magnetic field intensities (10, 1, 0.1, −0.1, −1, −10 kOe) at 300 K and 5 K, respectively. (d)–(e) MR curves measured at different angles. (f) Plot of the difference of device resistance under positive and negative saturation magnetic field with $\theta$.

## 4. Conclusion

We reported the observation of the partial asymmetric MR effect in the Pt/$HfO_{2-x}$/$NiO_y$/Ni heterojunction induced by the electric-controlled migration of oxygen and nickel ions for novel magnetic nanostructure establishment. The partial asymmetric MR effect was proposed to originate from the combined magnetic coupling effect of the $NiO_y$/Ni interface and nanofilaments of Vo and Ni. The MR behavior under different temperatures and angles was systematically studied, exhibiting good temperature stability and linear response to the magnetic field orientation. This device can find potential applications for magnetic direction detection and navigation applications. Our findings not only revealed the interesting low-dimensional magnetoelectric transportation behavior but also provided new versatile platforms for the design of next-generation high-performance and multifunctional nanodevices.

## Acknowledgements

Project supported by the National Key Research and Development Program of China (Grant No. 2021YFA1202600), the National Natural Science Foundation of China (Grant Nos. 92064011, 62174164, 61974179, and 61674153), Youth Innovation Promotion Association of the CAS (Grant No. 2020297), Natural Science Foundation of Zhejiang Province (Grant No. LR17E020001), Ningbo Natural Science Foundation (Grant No. 202003N4029), and C. Wong Educa-

tion Foundation (Grant No. GJTD-2020-11).

## References


[1] Zhao T, Scholl A, Zavaliche F, Lee K, Barry M, Doran A, Cruz M P, Chu Y H, Ederer C, Spaldin N A, Das R R, Kim D M, Baek S H, Eom C B and Ramesh R 2006 *Nat. Mater.* **5** 823

[2] Wang L, Wang D, Cao Q, Zheng Y, Xuan H, Gao J and Du Y 2012 *Sci. Rep.* **2** 223

[3] Zhu X, Zhou J, Chen L, Guo S, Liu G, Li R W and Lu W D 2016 *Adv. Mater.* **28** 7658

[4] Chen X, Zhu X, Xiao W, Liu G, Feng Y, Ding J and Li R W 2015 *ACS Nano* **9** 4210

[5] Chiba D and Ono T 2013 *J. Phys. D: Appl. Phys.* **46** 213001

[6] Ikeda S, Miura K, Yamamoto H, Mizunuma K, Gan H D, Endo M, Kanai S, Hayakawa J, Matsukura F and Ohno H 2010 *Nat. Mater.* **9** 721

[7] Mangin S, Ravelosona D, Katine J A, Carey M J, Terris B D and Fullerton E E 2006 *Nat. Mater.* **5** 210

[8] Meng H and Wang J P 2006 *Appl. Phys. Lett.* **88** 172506

[9] Song C, Cui B, Peng J, Mao H and Pan F 2016 *Chin. Phys. B* **25** 067502

[10] Matsukura F, Tokura Y and Ohno H 2015 *Nat. Nanotechnol.* **10** 209

[11] Chen Q, Liu G, Gao S, Yi X, Xue W, Tang M, Zheng X and Li R W 2019 *MRS Commun.* **9** 14

[12] Zhou X, Yan Y, Jiang M, Cui B, Pan F and Song C 2016 *J. Phys. Chem. C* **120** 1633

[13] Molinari A, Hahn H and Kruk R 2019 *Adv. Mater.* **31** 1806662

[14] Yang J J, Miao F, Pickett M D, Ohlberg D A, Stewart D R, Lau C N and Williams R S 2009 *Nanotechnology* **20** 215201

[15] He Z Y, Wang T Y, Chen L, Zhu H, Sun Q Q, Ding S J and Zhang D W 2019 *Nanoscale Res. Lett.* **14** 51

[16] Yang Y, Gao P, Gaba S, Chang T, Pan X and Lu W 2012 *Nat. Commun.* **3** 732

[17] Wang H and Yan X 2019 *Phys. Status Solidi RRL* **13** 1900073

[18] Changa C F, Chena J Y, Huanga G M, Lina T Y, Taia K L, Huanga C Y, Yehd P H and Wu W W 2018 *Nano Energy* **53** 871

[19] Lai Y F, Chen F, Zeng Z C, Lin P J, Cheng S Y and Yu J L 2017 *Chin. Phys. B* **26** 087305

[20] Pang H and Deng N 2014 *Chin. Phys. Lett.* **31** 107303

[21] Otsuka S, Hamada Y, Shimizu T and Shingubara S 2014 *Appl. Phys. A* **118** 613

[22] Li L, Liu Y, Teng J, Long S, Guo Q, Zhang M, Wu Y, Yu G, Liu Q, Lv H and Liu M 2017 *Nanoscale Res. Lett.* **12** 210

[23] Yang Z, Zhan Q, Zhu X, Liu Y, Yang H, Hu B, Shang J, Pan L, Chen B and Li R W 2014 *Europhys. Lett.* **108** 58004

[24] Xie Z, Gao S, Ye X, Yang H, Gong G, Lu Y, Ye J, Liu G and Li R W 2020 *Phys. Chem. Chem. Phys.* **22** 26322

[25] Zhao D, Qiao S, Luo Y, Chen A, Zhang P, Zheng P, Sun Z, Guo M, Chiang F K, Wu J, Luo J, Li J, Kokado S, Wang Y and Zhao Y 2017 *ACS Appl. Mater. Interfaces* **9** 10835

[26] Lee T S, Lee N J, Abbas H, Lee H H, Yoon T S and Kang C J 2020 *ACS Appl. Electron. Mater.* **2** 1154

[27] Wu X, Mei S, Bosman M, Raghavan N, Zhang X, Cha D, Li K and Pey K L 2015 *Adv. Electron. Mater.* **1** 1500130

[28] Aldana S, García-Fernández P, Rodríguez-Fernández A, Romero-Zaliz R, González M B, Jiménez-Molinos F, Campabadal F, Gómez-Campos F and Roldán J B 2017 *J. Phys. D: Appl. Phys.* **50** 335103

[29] Rodriguez-Fernandez A, Aldana S, Campabadal F, Suñé J, Miranda E, Jiménez-Molinos F, Roldán J B and Gonzalez M 2017 *IEEE T. Electron Dev.* **64** 3159

[30] Chen Y, Pourtois G, Adelmann C, Goux L, Govoreanu B, Degreave R, Jurczak M, Kittl J A, Groeseneken G and Wouters D J 2012 *Appl. Phys. Lett.* **100** 113513

[31] Zhang Y, Mao G Q, Zhao X, Li Y, Zhang M, Wu Z, Wu W, Sun H, Guo Y, Wang L, Zhang X, Liu Q, Lv H, Xue K H, Xu G, Miao X, Long S and Liu M 2021 *Nat. Commun.* **12** 7232

[32] Xue K H, Traoré B, Blaise P, Fonseca L R C, Vianello E, Molas G, Salvo B D, Ghibaudo G, Magyari-Kope B and Nishi Y 2014 *IEEE T. Electron Dev.* **61** 1394

[33] Huang T K, Chen J Y, Ting Y H and Wu W W 2018 *Adv. Electron. Mater.* **4** 1800256

[34] Tan T, Guo T, Wu Z and Liu Z 2016 *Chin. Phys. B* **25** 117306

[35] Russo U, Ielmini D, Cagli C and Lacaita A L 2009 *IEEE T. Electron Dev.* **56** 186

[36] Mei S, Bosman M, Nagarajan R, Wu X and Pey K L 2016 *Microelectron. Reliab.* **61** 71

[37] Li S, Plaskett T S, Freitas P P, Bernardo J, Almeida B and Sousa J B 1998 *IEEE T. Magn.* **34** 3772

[38] Carey M J and Berkowitz A E 1992 *Appl. Phys. Lett.* **60** 3060

[39] Rheem Y, Yoo B Y, Beyermann W P and Myung N V 2007 *Nanotechnology* **18** 125204

[40] Rheem Y, Yoo B Y, Koo B K, Beyermann W P and Myung N V 2007 *J. Phys. D: Appl. Phys.* **40** 7267

[41] Roy A, Toro J A D, Amaral V S, Muniz P, Riveiro J M and Ferreira J M F 2014 *J. Appl. Phys.* **115** 073904

[42] Agarwal S, Wang B, Yang H, Dhanapal P, Shen Y, Wang J, Wang H, Zhao J and Li R W 2018 *Phys. Rev. B* **97** 214427

[43] Singh S, Rawat R, Muthu S E, D'Souza S W, Suard E, Senyshyn A, Banik S, Rajput P, Bhardwaj S, Awasthi A M, Ranjan R, Arumugam S, Schlagel D L, Lograsso T A, Chakrabarti A and Barman S R 2012 *Phys. Rev. Lett.* **109** 246601